(NEW) WISPER(X) load spectra
Test results and analysis

OB_TG1_R024 rev. 000
doc. no. 10313

Draft version
Confidential

OPTIMAT BLADES

TG1

Rogier Nijssen

Change record

Issue/revision	date	pages	Summary of changes
draft (000)	Oct. 14, 2005		

1 Introduction

This report describes the load spectrum tests and predictions for OB standard MD coupons, of TG1 [1], done at WMC. These tests are designed to investigate effects of variable amplitude loading. Simple load spectra ('block tests') have also been done in this programme, and will be reported in [2].
We discuss the test set-up and programme in chapter 2, and present the results in chapter 0. The spectrum test results can be used to validate Miner's sum and the residual strength based life prediction, which is demonstrated in chapters 3.2 and 3.3.

2 Test set-up and test programme

In OptiDAT [3], the load spectrum tests are coded as (N/R)W(X), as indicated in table **1**.

Table 1: OptiDAT spectral test codes

W	WISPER
WX	WISPERX
N	New (WISPER or WISPERX)
R	Reversed (WISPER or WISPERX)

Table 2: Spectrum cycle content

	Integers				levels				
Spectrum	**min**	**max**	**zero stress**	**no. of cycles**	**cumulative levels**	**average segment length (in levels)**	**average level**	**max. at segment**	**min. at segment**
WISPER	1	64	25	132711	3612010	14	41	34482	123303
WISPERX	1	64	25	12831	487864	19	41	5298	13482
NEW WISPER	5	59	22	47735	1397142	15	34	95459	1

See figure 1 and table 2 for an impression of the (NEW) WISPER(X) cycle content, and [4, 5, 6] for detailed information about WISPER(X) and NEW WISPER. In table 2, a segment is bounded by an adjacent peak and valley. The characteristics are given in levels, where appropriate.
Spectrum tests were done on standard OPTIMAT MD and UD specimens (geometries R0300 and R0400), for details see [3]. The spectral tests were evenly distributed between the laboratories of DLR and WMC. UP and CRES have also planned spectrum testing.
At WMC, they were carried out on a 100 kN Instron frame using the Fastrack Random version 7.4.1 software. Essentially, spectrum loading software is designed to interpolate a sequence of peaks and valleys from an input file with a sine or triangular waveshape and load the specimen accordingly. The spectrum input files are scaled by varying the load level of the maximum peak. The loading rate is scaled accordingly. The loads and loading rates were predetermined using a Miner-based routine taken from [7, 8], and prescribed in [9]. (Maximum) loading rate was constant for a single spectrum. The loading rate for the spectral tests (ca. 400 kN/s) is in general smaller than for the constant amplitude data, and heating of the specimen is likely to occur less than in constant amplitude testing. This is confirmed by temperature measurements on the side-surface of the specimen near the tab.
Force range, displacement range, and strains were measured (the latter using a standard OB clip-gauge in a back-to-back configuration) prior to the test and during the test. In addition, deviations from the command value were tracked and recorded in a separate log file.

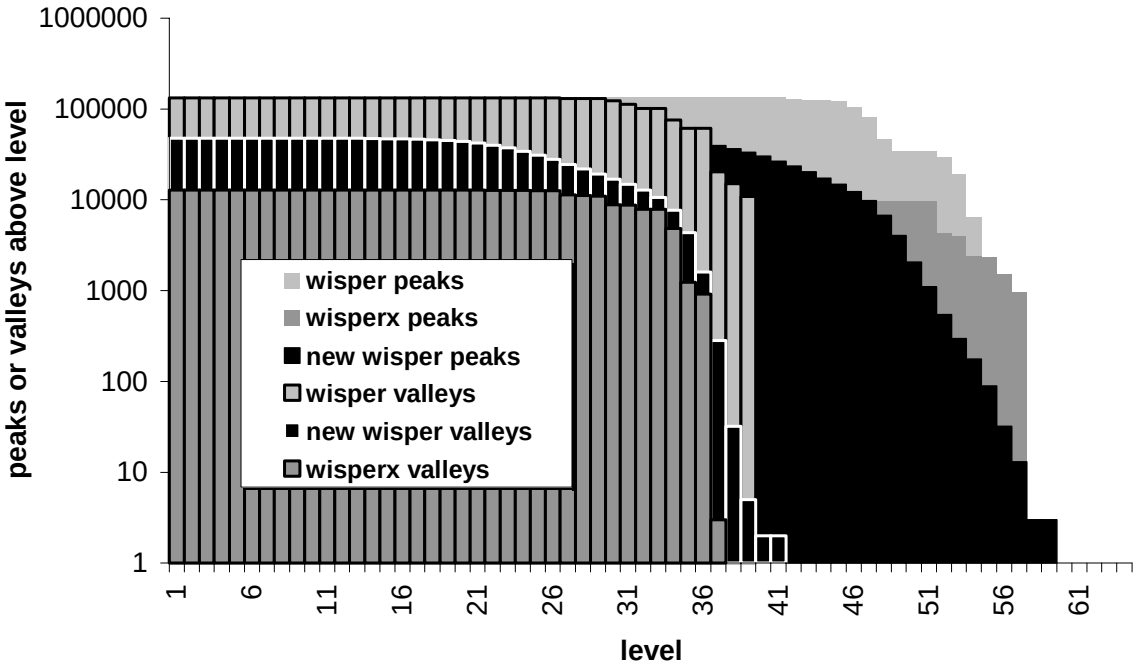

Figure 1: (NEW) WISPER(X) cycle content

3 Results and analysis

This chapter gives the tabulated results for (NEW) WISPER(X) tests on MD, and compares them to predictions using Miner-based approaches and a strength degradation based life prediction.

3.1 Overview of the results

The test results are presented in table 3. Results are or will be reported in OptiDAT [3].

Table 3: Spectrum load test results for WMC

Name	thickness	width	Type	level	F_{max}	s_{max}	cycles	sequences	failure segment	loading rate	E_t	E_c
	mm	mm	-	-	kN	MPa	-	-	-	kN/s	GPa	GPa
GEV206_R0300_0872	3.66	24.96	W	1	42.58	467	1082895	8.16	42414	291.72	43.625	44.645
GEV206_R0300_0884	3.63	25.08	W	1	42.76	470	512353	3.86	228439	292.95	44.225	46.125
GEV206_R0300_0915	3.63	25.05	W	1	42.66	471	374137	2.82	217429	292	44.35	
GEV206_R0300_0354	3.70	25.47	W	3	34.34	365	4783996	36.05	12800	377.83	42.3	42.69
GEV206_R0300_0861	3.60	25.06	W	3	33.78	375	3319644	25.01	3738	371.67	43.795	43.49
GEV206_R0300_0880	3.55	24.91	W	3	33.55	381	3996801	30.12	30942	369.15		
GEV206_R0300_0890	3.57	24.99	W	3	30.56	343	8744079	65.89	235728	369.79		
GEV206_R0300_0899	3.59	25.30	W	3	33.92	378	3188805	24.03	7482	373.3	43.76	44.035
GEV206_R0300_0928	3.59	24.98	W	3	31.34	350	5577893	42.03	8062	368	43.595	44.62
GEV207_R0400_1034	6.80	25.03	NW	3	40.11	236	5655934	118.49	46408	423.34	29.68	30.225
GEV207_R0400_1042	6.75	24.87	NW	3	39.82	238	3198227	67.00	95433	420.21	29.535	30.41
GEV207_R0400_1075	6.71	25.05	NW	3	40.14	239	3771043	79.00	95426	423.68	29.815	30.585
GEV207_R0400_1076	6.76	25.09	NW	3	40.21	237	2386734	50.00	95438	424.35	28.97	29.195
GEV207_R0400_1022	6.85	24.99	NW		45.2	264	1286745	26.96	91270	422.58	26.74	26.885
GEV207_R0400_1050	6.77	25.10	NW		45.34	268	707841	14.83	79102	423.85	27.945	28.02
GEV207_R0400_1039	6.78	24.91	W	1	53	314	460994	3.47	125722	357.92	28.71	29.04
GEV207_R0400_1044	6.69	25.01	W	1	53.25	319	559042	4.21	56396	359.57	29.895	30.535
GEV207_R0400_1055	6.75	24.96	W	1	53.16	316	866723	6.53	140914	359.03	29.585	29.89
GEV207_R0400_1068	6.76	24.96	W	1	53.13	315	825533	6.22	58534	358.78		30.87
GEV207_R0400_1052	6.80	24.95	W	3	42.1	249	12291879	92.62	164934	451.46	28.585	29.555
GEV207_R0400_1078	6.80	25.09	W	3	42.39	249	9705199	73.13	34592	454.54		31.185
GEV207_R0400_1015	6.76	25.41	W		46.08	267	7061136	53.21	54906	430.78	27.67	27.825
GEV207_R0400_1036	6.84	25.00	WX	3	42.24	247	3222248	251.13	3334	452.91	27.41	27.52
GEV207_R0400_1056	6.23	25.08	WX	3	43.27	277	275130	21.44	11358	454.36	29.945	30.095
GEV207_R0400_1057	6.78	25.00	WX	3	42.25	249	2094311	163.22	5716	453	27.19	27.235
GEV207_R0400_1083	6.86	24.98	WX	3	42.21	246	2889312	225.18	4674	452.64		31.185

As is clear from table 2, there are two most likely candidate segments for failure in the WISPER(X) spectra; the maximum peak and minimum valley. Most of the specimens subjected to WISPER(X) did not fail exactly at these locations. However, it is possible that the terminal damage, leading to failure, initiated at these peaks. If more tests are performed, statistical evidence can be collected

whether failure is more prevalent around the maximum peaks and valleys or not. Most of the NEW WISPER tests failed at the maximum peak, which coincides with the end of the sequence.

3.2 Life predictions using Miner's sum

A spreadsheet tool was created to perform a life prediction using Miner's sum. A similar tool is uploaded on the website [10]. This tool uses the log-log representation of the S-N curve, and the CLD for MD material was created from representative OptiDAT data [3], finding the S-N parameters using linear regression (for parameters, see table 4). For the main R-ratios, the parameters of the S-N curve are also reported in [11]. The tool can be used to investigate the influence of changes in the S-N curve parameters and Miner formulation on the WISPER(X) prediction.

Table 4 : a and b parameters
from $log(N)=a log(s)+b$
(for standard OB MD)

R	a	b
-1	-9.01	24.91
0.1	-9.13	26.73
10	-23.21	62.03
0.5	-8.34	25.40
-2.5	-14.37	33.35
-0.4	-8.02	23.37

(UTS: 530 MPa; UCS –461 MPa)

The resulting CLDs are shown in figures 2-4. Three different CLDs are used, viz:

- Linear Goodman Diagram
- Shifted Goodman Diagram
- CLD built from multiple R-ratios

Prediction results and the preliminary results are given in figures 5-7 for the three spectra tested until now. The predictions are made using the Rainflow counted spectra, and using the CLD interpolation methods also described in [12].
Predictions for WISPER and WISPERX do not show much difference if they are made using a (shifted) Linear Goodman Diagram. This was also noted in previous work done at WMC [13]. However, the difference in cycle content is of influence on the life prediction when the detailed information in the multiple R-ratio CLD is used, see figure 5 and 6. This underlines the importance of a detailed CLD for the accuracy of the life prediction.

Note, that the shifted Goodman diagram, as prescribed by the newest version of the Germanischer Lloyd guidelines (GL) [14], yields the longest, least conservative, lifetimes, when compared to the classical Linear Goodman Diagram (e.g. prescribed in [15]). Taking into account a detailed description of the constant life diagram, using S-N definitions at multiple R-ratios, gives a more conservative prediction. In fact, the latter prediction is in best agreement with the experimental data obtained thusfar.

3.3 Life prediction using residual strength degradation

Life prediction was also done using a residual strength degradation model. The model and procedure for parameter estimation are described in detail in [16]. The model was implemented into a computer programme, that carries out a segment-by-segment analysis of strength degradation.

The strength degradation algorithm used in this chapter is shown in the flow-chart of figure 8. Note, that the prediction consists of two main procedures. In the first part is the pre-processing stage. The spectrum is processed once and analysed in terms of range, mean level per cycle, R-ratio, number of cycles to failure, etc. This information is stored for later use in phase 2. In this second phase, the actual strength is monitored. Per cycle, the strength degradation is calculated using the information obtained in phase 1, and from the strength degradation prior to the cycle.

The same CLDs as used in the previous chapter were used here. In addition, the strength degradation behaviour of the material was assumed to be linear for tensile, and 'sudden death' for compressive strength. From the strength degradation data obtained in the project up to now, this is the general strength degradation trend, actually for most of the different materials tested. 'Early failure' was not noticed in any strength degradation test set. Figure 9 shows the schematic strength degradation behaviour noticed in the OPTIMAT residual strength programme, and also reported in [16].
In the one-parameter strength degradation model, for the current predictions, tensile strength degradation was modeled using a strength degradation parameter of 1; compressive strength by a value of the strength degradation parameter of 10.
The prediction results for the tested spectra are shown in figure 10-12, together with Miner based predictions. Thus, a thorough comparison can be made of the benefits of the strength degradation model compared to Miner's sum, and of using a more detailed CLD compared to the relatively simple Linear and Shifted Goodman Diagrams.
Although the CLDs are the same, there is one minor discrepancy between the Miner-based life prediction and the strength-based life prediction. Strictly speaking, the life prediction using Miner's sum and the prediction using the strength degradation method may not be directly compared. The reason is, that the counting methods used to quantify the cyclic content of the spectrum are different. In the Miner prediction, the sequence was Rainflow counted, whereas in the strength degradation prediction, the cycles were effectively characterised in terms of a range-mean count. However, in the figures including the strength-based life prediction, the Miner predictions are also based on the range-mean count of the spectrum. Comparing these predictions to figures 5-7, the difference in life prediction based on differences in counting methods is very limited, especially for the full CLD with 6 R-ratios. For instance, compare 'Multiple R-ratio (6 R-ratios)' in figure 5 to 'Multiple R-ratio (6 R-ratios)' in figure 10. Both lines are at virtually the same location, even though the Miner prediction of figure 5 was based on a Rainflow counted sequence, and the Miner prediction of figure 10 was based on a range-mean count.

It is clear from the figures, that the strength degradation model, although it is far more computationally intensive, and requires considerable experimental effort in completing the strength degradation characterisation for various load characteristics, is not significantly better in predicting life than the Miner based approach. One should take into account, that, as the strength degradation parameter approaches infinity, the strength degradation based life prediction approaches the Miner-based prediction. Apparently, using strength degradation parameters of 1 and 10 for tensile and compressive strength, only shifts the prediction by a factor of at most 2. More significant shifts in the residual strength based life predictions can be achieved by choosing a strength degradation parameter much smaller than 1, as is illustrated in the illustrative example prediction of figure 13. However, this type of residual strength behaviour is far besides experimental experience.

Not only does the above lead to the conclusion, that residual strength based life predictions are of no use in the cases investigated, these findings also feed suspicion that influential sequence effects in the load spectra investigated here are absent.

4 Concluding Remarks

- Test results were predicted by the classical fatigue analysis and using a residual strength model.
    - Miner's sum predictions, as well as residual strength life predictions are extremely sensitive to the parameters of the S-N curve. The influence of S-N parameters can be more important than the actual fatigue model used (Miner or Residual Strength).
    - Life predictions using a Linear or shifted Linear Goodman diagram give longer lives than using the detailed CLD for the spectra investigated. In fact, they are highly non-conservative. The detailed CLD yields predictions that are in better agreement with the experimental data. This underlines the importance of having an accurate material constant amplitude fatigue description.
    - Life predictions using the Shifted Goodman Diagram (GL 2003, [14]) give an even more non-conservative prediction than using the Linear Goodman Diagram (GL 1999 [15]), for the tensile spectra investigated. It is expected, that for a compressive spectrum the GL 2003 formulation will be more conservative.
    - Counting method (Rainflow or range-mean) is of no great influence on life prediction, although Rainflow method generally gives more conservative life estimates

- Strength degradation based life prediction does not seem to be promising compared to Miner-based predictions
- Sequence effects in the spectra investigated are likely to be non-existent or insignificantly small.

5 References

1. Kensche, Ch., Krause, O., Söker, H., Nijssen, R., *'Detailed Plan of Action for WP3 and WP4'*, OB_TG1_O002, rev 6, doc. no. 10053, sept 2005
2. Nijssen and Krause, block test report, under construction
3. Nijssen, R.P.L., 'Optidat -database reference document-', OB report OB_TC_R018, doc. No. 10224, 2004
4. ten Have, A.A., 'WISPER and WISPERX - Final definition of two standardised fatigue loading sequences for wind turbine blades', 1992)
5. ten Have, A.A., 'WISPER and WISPERX - a summary paper describing their background, derivation and statistics', 1992
6. Bulder, Bernard, Peeringa, Johan M., Lekou, Denja, et al., 'NEW WISPER - Creating a New Load Sequence From Modern Wind Turbine Data', OPTIMAT BLADES report OB_TG1_R020, doc. No. 10278, 2005
7. Brøndsted, Povl, Andersen, Svend Ib, Lilholt, Hans, 'Fatigue damage accumulation and lifetime prediction of GFRP materials under block loading and stochastic loading', proc. 18th International Symposium on Materials Science: Polymeric Composites - Expanding the limits, eds: S.I. Andersen, P. Brøndsted, H. Lilholt et al., 1997, pp. 269-278
8. Dover, W.D, 'Variable Amplitude Fatigue of Welded Structures', In: Fracture Mechanics: Current Status, Future Prospects. R.A. Smith (Ed.), Pergamon Press, Cambridge, 1979, pp. 125-147
9. Krause, O., 'Test specification for load spectra tests', OB report OB_TG1_R021, doc. no. 10280_001, 2005
10. Nijssen, R.P.L., 'WISPER(X) life prediction for OB MD laminate (spreadsheet tool)', OB_TC_O007, doc. no. 10276, 2005
11. Nijssen, R.P.L., Lekou, D., 'OptiDAT data summary -strength and life of standard OB specimens- ', OB report OB_TG1_R022 rev 001, doc. no 10284, 2005
12. Nijssen, Rogier, Krause, Olaf, Philippidis, Theodore, 'Benchmark of lifetime prediction methodologies', OPTIMAT report: OB_TG1_R012, doc. No. 10218, 2004
13. van Delft, D.R.V., de Winkel, G.D., Joosse, P.A., 'Fatigue behaviour of fibreglass wind turbine blade material under variable amplitude loading', proc. AIAA/ASME Wind Energy Symposium, no. AIAA-97-0951, 1997, pp. 180-188
14. Germanischer Lloyd, 'Guideline for the Certification of Wind Turbines', 2003
15. Germanischer Lloyd, 'Guideline for the Certification of Wind Turbines', 1999
16. Nijssen, R.P.L., Passipoularidis, V., Smits, A., et al., 'Residual Strength Tests -data and analysis-', OB report OB_TG5_R007, doc. no. 10285, 2005t

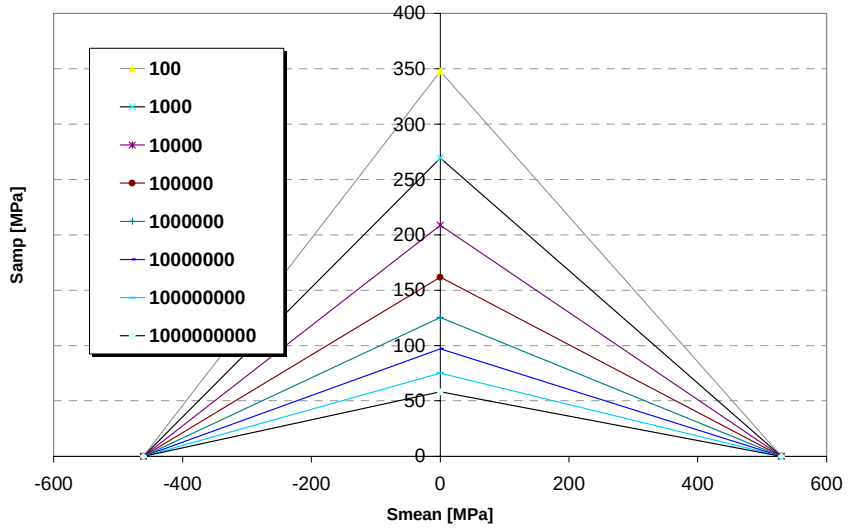

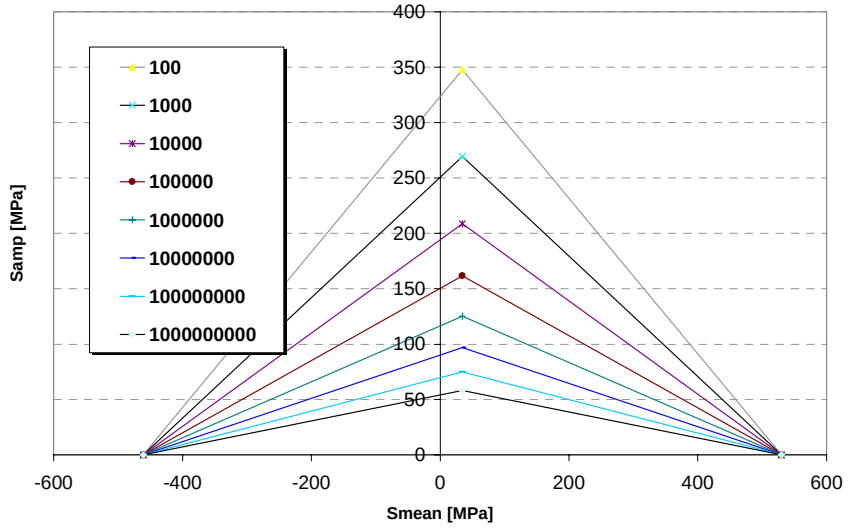

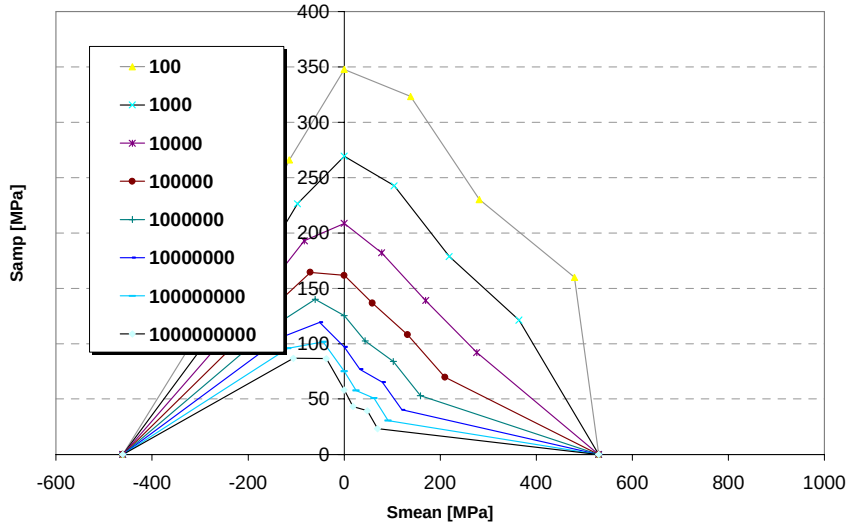

Figure 2-4: Linear Goodman Diagram, Shifted Linear Goodman diagram and detailed CLD for MD

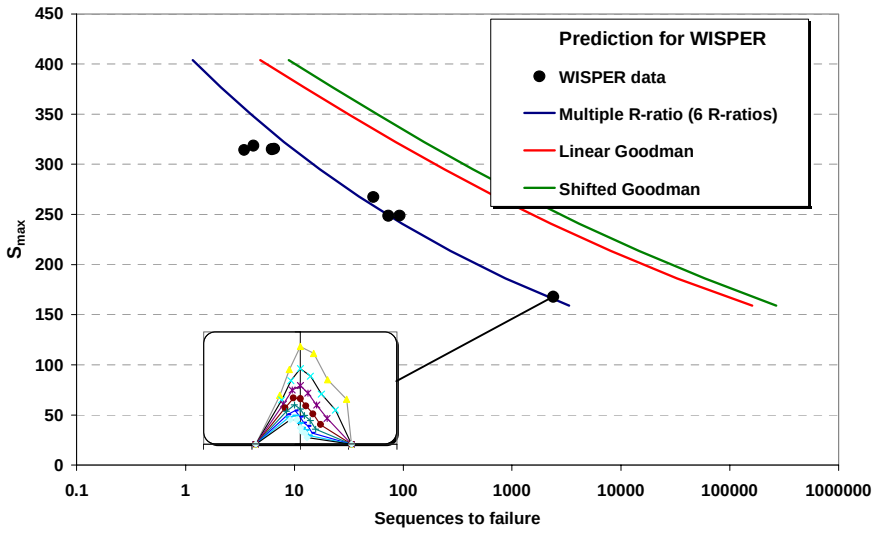

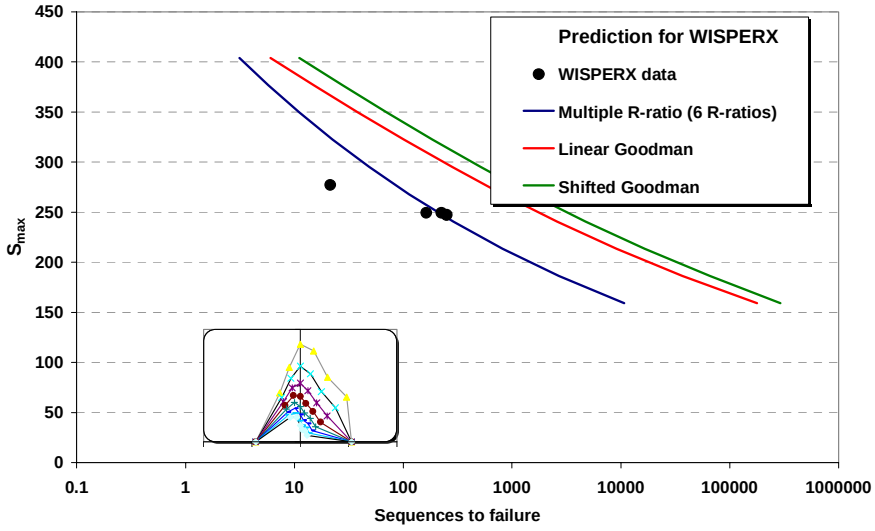

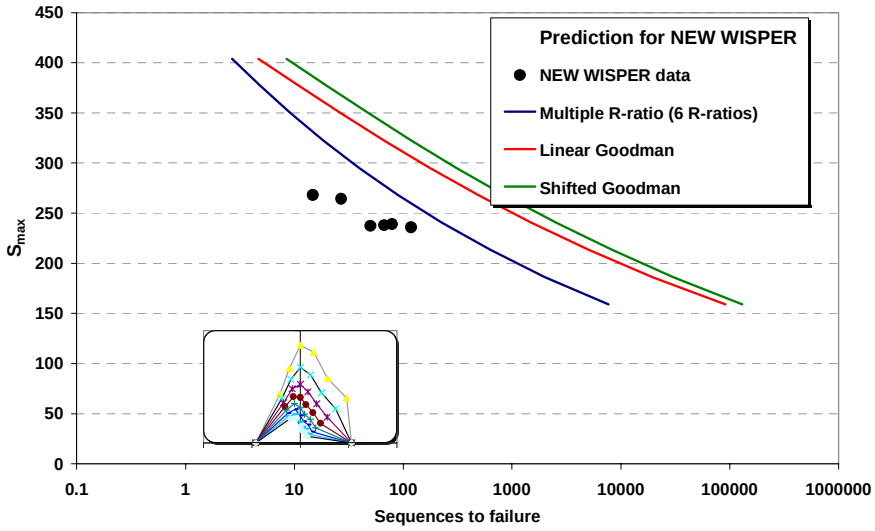

Figure 5-7: Miner-based predictions for WISPER, WISPERX and NEW WISPER

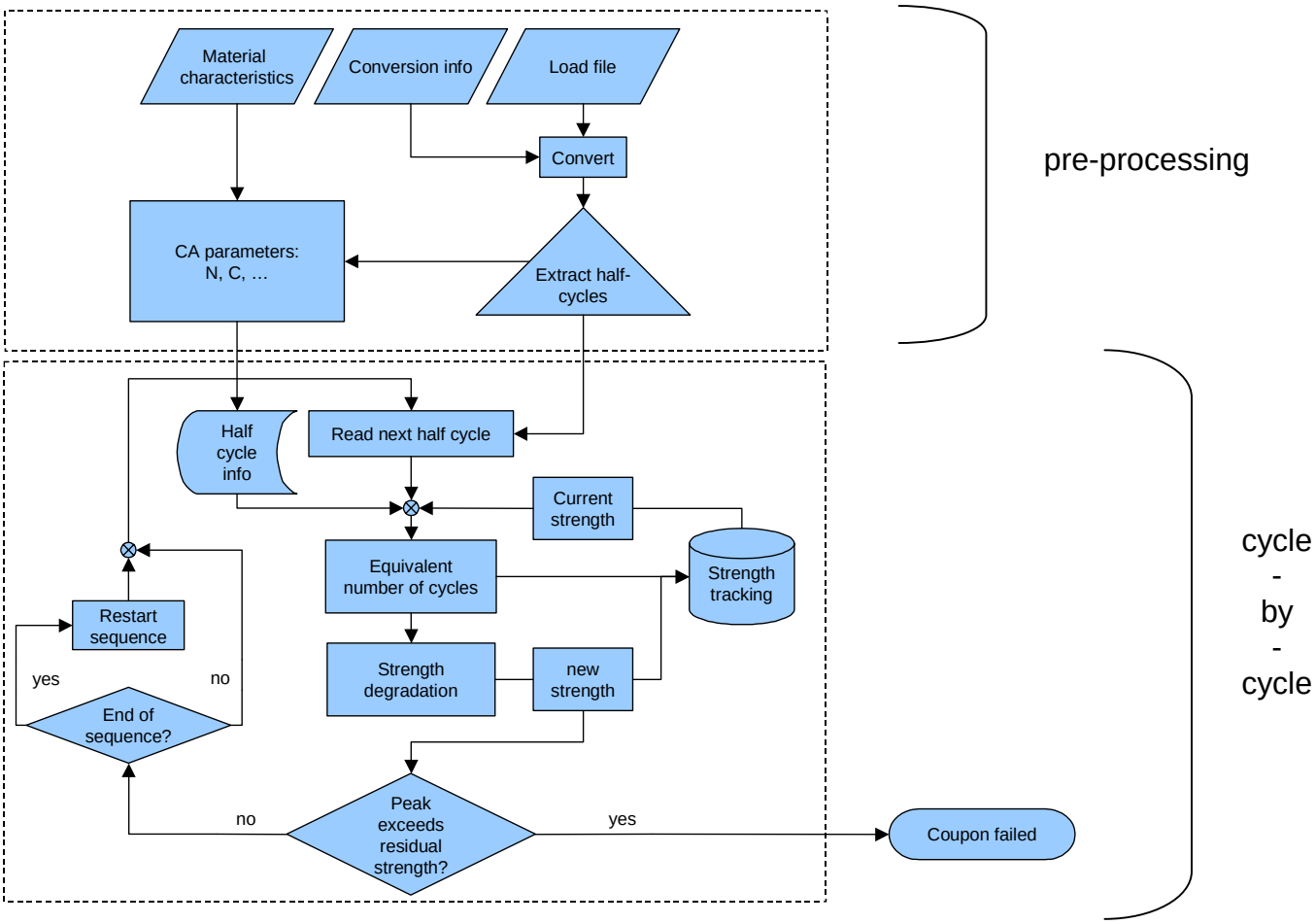

Figure 8: Flow-diagram for segment-by-segment strength degradation based life prediction

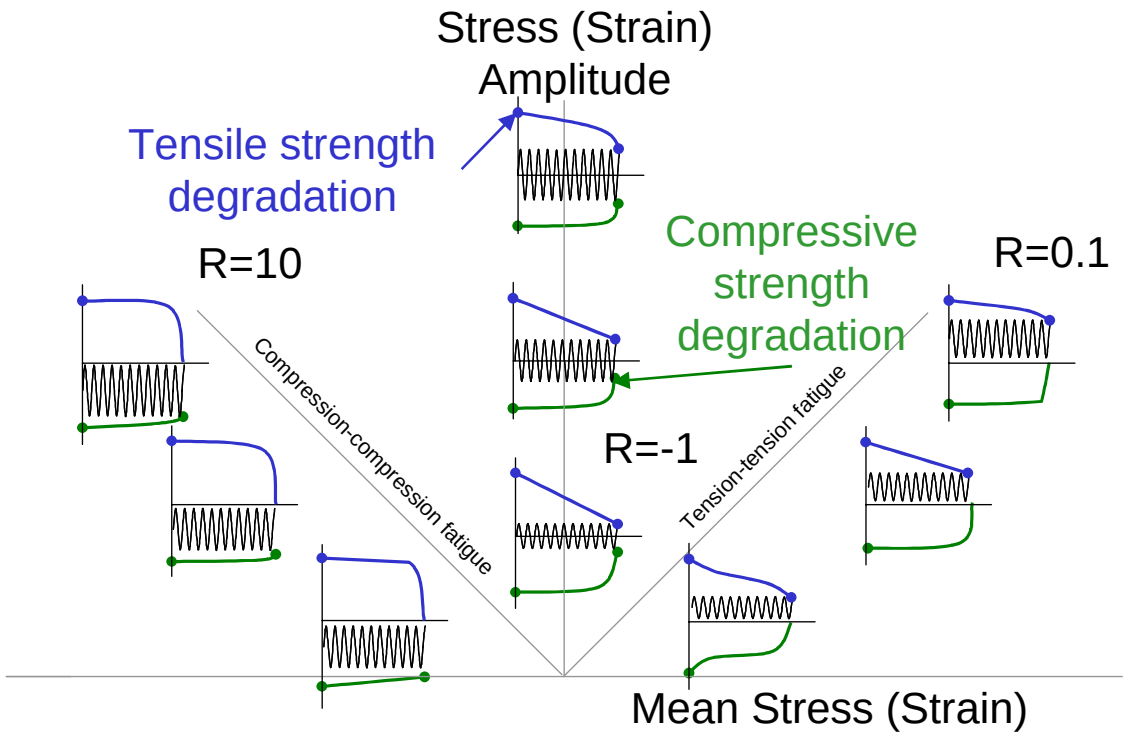

Figure 9: General, schematic, strength degradation behaviour of OPTIMAT materials

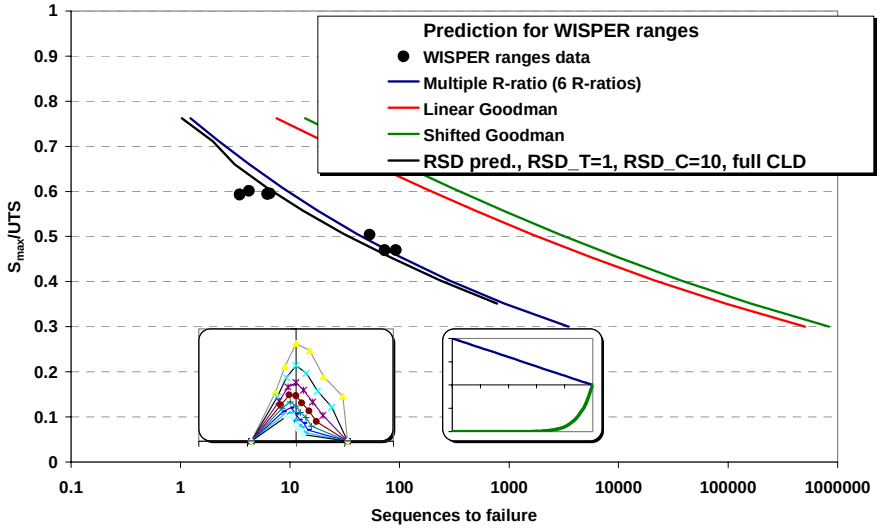

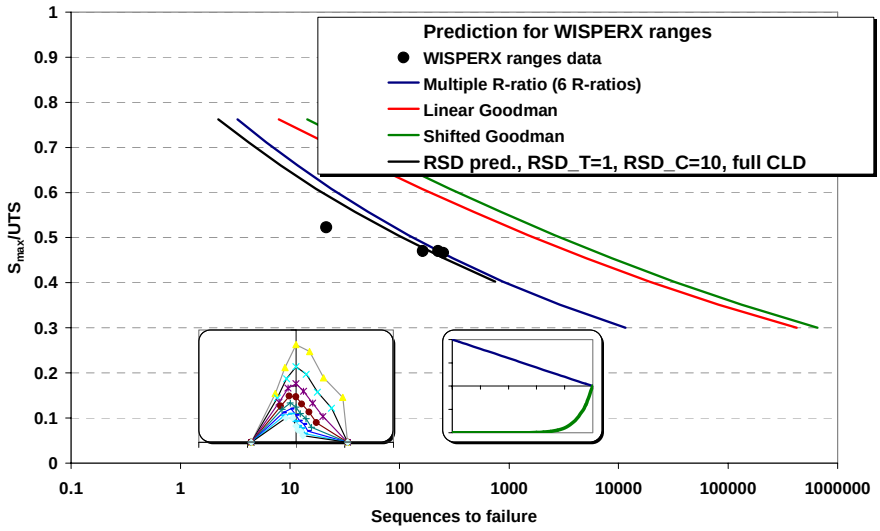

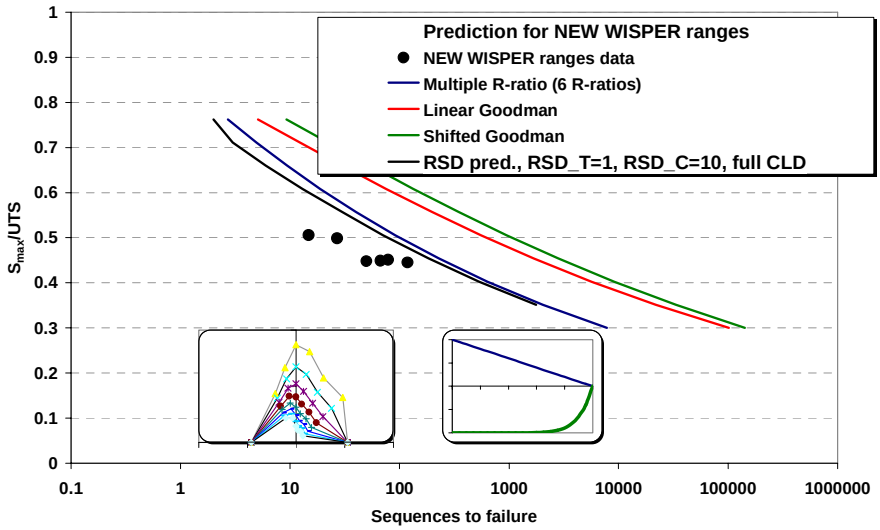

Figure 10-12: General strength degradation behaviour of OPTIMAT materials

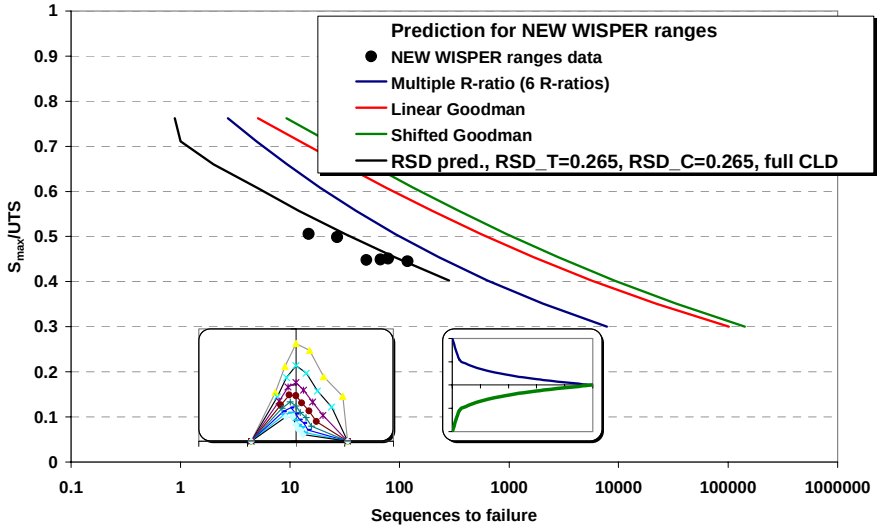

Figure 13: Strength degradation life prediction using unrealisticly low value of strength degradation parameter